4.2 **FINE SCALE INITIALIZATION AND PREDICTION OF CONVECTIVE SYSTEMS OVER FRENCH MOUNTAINOUS AREAS.**

Didier Ricard*, Véronique Ducrocq and Jean-Philippe Lafore.
CNRM, Météo-France, Toulouse, 31057, France.

## 1. INTRODUCTION

Both static and dynamic initializations are investigated for numerical prediction of convective events at high resolution. In this study, we focus on mesoscale convective systems that generate large rainfalls over French mountainous areas. As a consequence, these intense events can produce devastating and deadly flash floods. The forecast of these convective events is generally problematic for the operational models.

With the intention of improving the high resolution numerical simulations of these convective cases, we concentrate on the problem of model initialization by evaluating different initialization methods:

- a fine scale initialization using mesoscale surface data analyses and simple cloud and precipitation analyses derived from conventional radar and infrared satellite data,
- a dynamic initialization by Newtonian relaxation (nudging) using mesoscale analyses.

We compare the results to a classic way of initialization of high resolution numerical models which consists of a simple dynamic adaptation from a larger scale operational analysis.

In this paper, we present the results of these different initialization methods for the prediction of a significant precipitation event.

## 2. CASE STUDY

The large precipitation have been induced by a convective system that occurred over the Massif Central (South of France) during autumn 1995 (13-14 October). It began around 21 UTC 13 October. It was quasi-stationary and it maintained more than 9 hours over the relief before dissipating and drifting towards the east. This event was characterized by heavy precipitation in a very localized area with observations reaching 262 mm in 11 hours. During its mature phase, this event looked like a V-shape regenerative convective system. The interaction between the orography and the low-level southeasterly flow moistened and warmed by Mediterranean sea is a key factor: the orographic forcing certainly played a preponderant part for triggering and maintaining this system, the low-level flow provided humidity and energy necessary to fuel the system. There was a weak synoptic forcing so a good description of mesoscale features is certainly needed for insuring a better prediction of this kind of system.

## 3. GENERAL DESCRIPTION OF THE NUMERICAL EXPERIMENTS

The high resolution numerical simulations have been carried out with the 3D mesoscale non-hydrostatic model MESO-NH (Lafore *et al*, 1998). It uses nested domains with two-way interaction. Two models have been employed in our experiments: a coarse mesh model with a 10 km horizontal resolution over a 960×1440 km² domain and a nested fine mesh model with a 2.5 km resolution over a 250×375 km² domain. This inner model is centered on the convective system. The coarse model uses a convection parameterization while the convective structures are explicitly resolved by the fine mesh model. The microphysical scheme includes predictive equations for six atmospheric water categories: water vapor, non-precipitating and precipitating liquid water, snow, non-precipitating ice and graupel (Stein *et al*, 2000).

| Experiment | Type of initialization | | | Initial time of the simulations |
|---|---|---|---|---|
| | Static | | Dynamic | |
| | Surface mesonet observations analysis | Humidity and hydrometeor fields adjustment | Nudging towards mesoscale analysis (1800-1900-2000-2100UTC) 3 hour preforescast period | |
| ADAP18 | NO | NO | NO | 1800 UTC |
| ANA22ADJ | YES | YES | NO | 2200 UTC |
| ANA22 | YES | NO | NO | 2200 UTC |
| ANA21 | YES | NO | NO | 2100 UTC |
| NUD18LC | NO | NO | YES ($G=3\times10^{-4}$ W=1) | 1800 UTC |
| NUD18LV | NO | NO | YES ($G=3\times10^{-4}$ W variable) | 1800 UTC |
| NUD18HC | NO | NO | YES ($G=6\times10^{-4}$ W=1) | 1800 UTC |
| NUD18HV | NO | NO | YES ($G=6\times10^{-4}$ W variable) | 1800 UTC |

***Table 1:*** *Description of experiments (See text for definition of G and W)*

* *Corresponding author address:* Didier Ricard, CNRM, Météo-France, 42, Av. G. Coriolis, 31057 Toulouse, France; e-mail: didier.ricard@meteo.fr

## 4. STATIC FINE SCALE INITIALIZATION

We first tested a static fine scale initialization method that makes use of surface observations and of radar and satellite data. This fine scale initialization has been developed and has proved its usefulness on convective cases that have occurred over flat terrain regions. We tested here its utility over more mountainous areas. The details of this fine scale initialization can be found in Ducrocq *et al* (2000). Only a brief summary is given here. This method is composed of two consecutive steps:

- Surface mesonet observations are analyzed with an optimal interpolation scheme tuned for the mesoscale (Calas *et al*, 2000). That component improves the meso-$\beta$ scale description of low-level conditions.

- A simple cloud analysis based on conventional radar reflectivities and infrared satellite data helps to adjust the humidity and hydrometeor fields of the initial state in the fine mesh model. The mixing ratio of water vapor and some hydrometeor fields (precipitating liquid water and snow) are modified: saturation is imposed inside the cloudy area (determined from infrared brightness temperature and radar reflectivities) and inside each rainy column (determined from radar reflectivities) precipitating liquid water is introduced below freezing level and snow is imposed above it. This component supplies a meso-$\gamma$ scale information about the presence of a developing convective system.

The fine scale initialization is applied one hour after the onset of the convective system: so, for the ANA22ADJ experiment, the complete fine scale initialization is applied at 22 UTC (see Table 1). The ANA22 experiment tests the sensitivity to the use of the second step of the initialization procedure; *i.e.* for this experiment, only the surface mesonet data analysis of the initialization is performed. Results are also compared to a classic dynamic adaptation from the 18 UTC large scale ARPEGE analysis (ADAP18 experiment).

**ADAP18 experiment:** For the ADAP18 simulation, the model fails to produce any well developed convective system. The surface rainfall amounts are very weak (31 mm) (Fig 2a) and the precipitating cells are confined to a small vertical extension (below 6 km). Figure 1 displays the bias and rms scores for all the experiments. The high bias value (-2.4 mm) shows a precipitation deficit for this simulation (Fig. 1). Detailed description of low-levels and in particular of the humidity field which is lacking in the large scale initial state seems crucial for triggering and maintaining the convective systems. Indeed, this humidity deficit is confirmed by a deficit of precipitable water contents (6 kg/m²) in the large scale analysis relative to the mesoscale analysis.

**ANA22ADJ experiment:** Results are significantly improved in this experiment compared to the ADAP18 experiment: the ANA22ADJ experiment reproduces this convective event at about the right location with its steady state character. The extension of simulated system and the accumulated precipitation maximum are comparable with observations (Fig. 2b,e). There is a 30km shift to the east in the northern part of the system, but the band structure of the system is well represented. The maxima of rainfall totals are well localized and close to the observed values: 99 mm to compare with the observed maximum of 135 mm (Fig. 4). Bias (-0.2 mm) and rms (10.4 mm) scores confirm the superiority of the ANA22ADJ experiment (Fig. 1).

**ANA22 experiment:** The ANA22 experiment also succeeds in simulating a convective system. Contrary to what has been established for simulation of convective system over flat terrain, the moisture and hydrometeor fields adjustment is not essential for triggering and maintaining these systems: the triggering of this system over the relief is insured by orographic forcing. However, the maxima of surface rainfall total are slightly weaker for ANA22 experiment in comparison with the results of the ANA22ADJ experiment (Fig. 4), moreover the bias (0.4 mm) and rms (11.7 mm) are higher (Fig. 1).

We have obtained very similar conclusions for another convective case over the same area (Ricard *et al*, 2000). The fine-scale initialization produces well developed systems and leads to better precipitation forecasts.

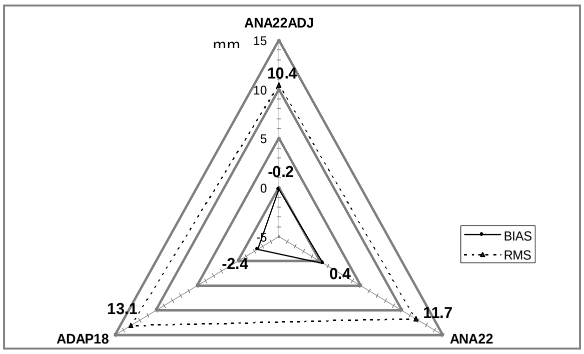


***Figure 1:*** *Bias and rms scores for the 5-h precipitation from 0100 to 0600UTC 14 October 1995 for experiments ADAP18, ANA22ADJ and ANA22. (Bias is in black solid line and rms in black dashed line. The grey lines label the graph every 5 mm, beginning at –5 mm.)*

## 5. DYNAMIC INITIALIZATION

Considering the benefit of the use of mesoscale analyses and in a lesser extent of moisture and microphysical adjustment in the previous static initialization, we have tried to develop a dynamic approach that makes use of those.

So, we have developed a sequential data assimilation based on the nudging technique (Hokes and Anthes 1976; Stauffer and Seaman, 1989). The implementation of this technique is quite simple and computational cost is relatively low. The basic idea is to relax during a preforecast integration period some prognostic model variables towards their observed or analyzed values.

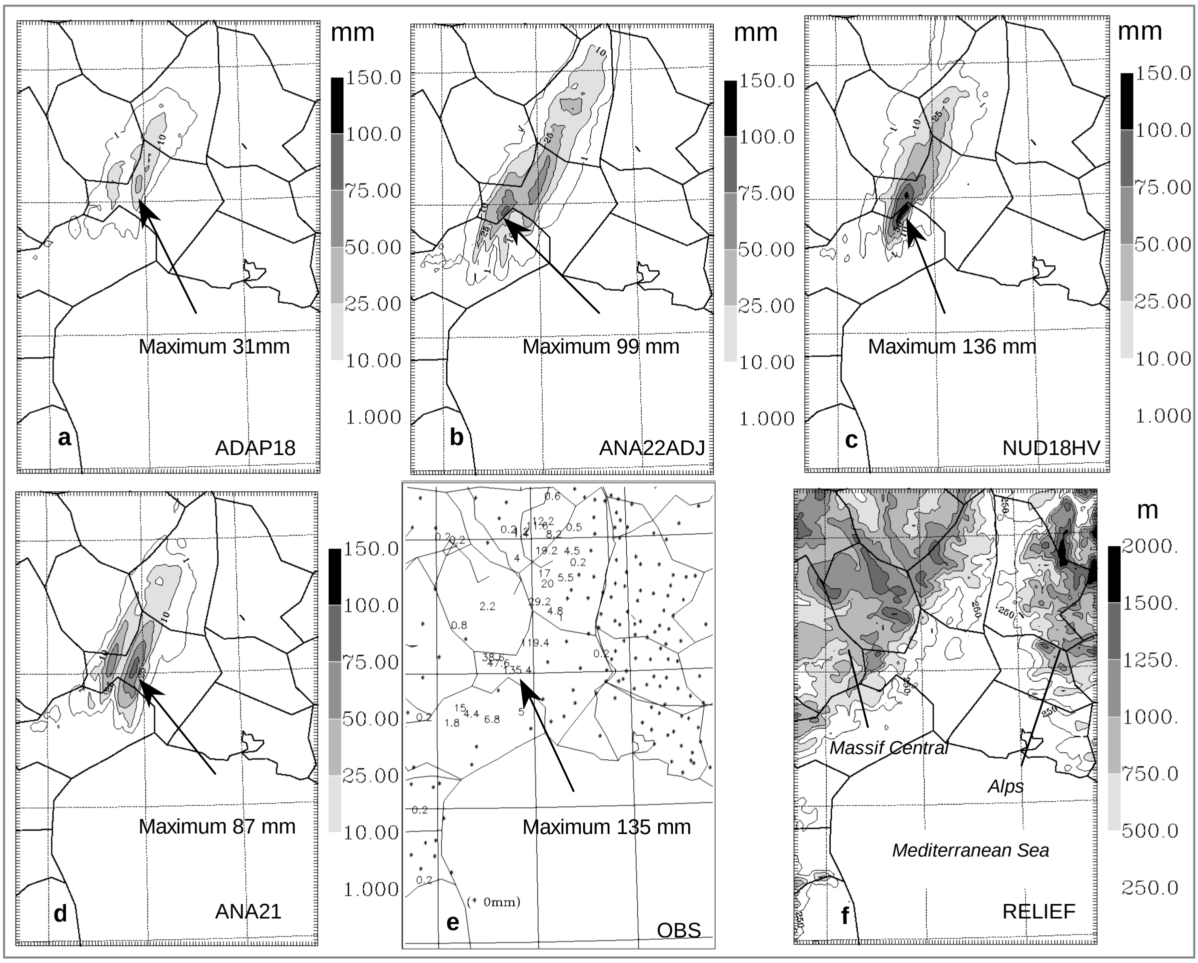


***Figure 2:*** *Forecast and observed 5-hour precipitation for 0100-0600 UTC 14 October 1995: ADAP18 (a), ANA22ADJ (b), NUD18HV (c), ANA21 (d), observations (e). Geography and orography in meters (f).*

As a first step, we nudge only towards mesoscale analyses. These variables are relaxed during a 3-h period towards mesoscale analysis, according the following equation:

$$\frac{\partial \alpha_M}{\partial t} = F(\alpha, \vec{X}, t) + G_\alpha \cdot W(\vec{X}, t) \cdot (\alpha_A - \alpha_M)$$

where:

$\alpha_M$ being a model prognostic variable and $\alpha_A$ the corresponding analyzed field interpolated for the same time; F for the total temporal evolution provided by the numerical model; $G_\alpha$ for the nudging coefficient and W for a space-time weighting function.

Here, the nudging term is added to the prognostic equations of horizontal wind (u,v), specific humidity (qv) and potential temperature ($\theta$). The analyzed fields are computed as a linear interpolation between the two nearest mesoscale analysis times (at one-hour intervals). We have tested different values for the nudging coefficient and different space-time weighting functions (Table 1). We have used nudging coefficient values comparable to those used in Wang and Warner (1988), *i.e.* G = $3\times10^{-4}$ $s^{-1}$ for NUD18LC and NUD18LV and a stronger coefficient G = $6\times10^{-4}$ $s^{-1}$ for NUD18HC and NUD18HV. We have used a constant weighting function W = 1 for NUD18LC and NUD18HC. As the mesoscale analyses are better over land rather over sea and within the PBL (because incorporating mainly surface land station data), we have tested a weighting function that decreases with altitude and over sea with the distance to the land in NUD18LV and NUD18HV experiments. By using this variable weighting function, the nudging is less intense in data-sparse regions (W = 0 over open sea and in the free atmosphere).

All the nudging experiments use a large scale analysis as initial state like the ADAP18 experiment does, so we can assess the benefit of nudging toward mesoscale analyses in comparison with the classic dynamic adaptation performed in ADAP18 experiment. To assess the benefit of the nudging 3-hour preforecast integration period, we have compared with a static initialization experiment (ANA21) that starts from the mesoscale analysis at 21 UTC, *i.e.* corresponding to the time of the end of the nudging preforecast period.

All the nudging experiments give better results than the ADAP18 experiment. The localization and the extension of the precipitation area are rather the same but we obtain better quantities for the nudging experiments. This is also confirmed by the bias and rms scores which are globally better for the nudging experiments (Fig. 3) and the maxima of precipitation are higher (Fig. 4). Among the nudging experiments, it is the NUD18HV experiment that gives the best results: the location and the extension of the precipitation area are very close to the observed ones, even for the northern part of precipitation pattern, the quantities are improved too (Fig. 2c). The other nudging experiments underestimate the precipitation (Fig. 4), that explains the high values of bias and rms scores for these experiments (Fig. 3). So a higher value of coefficient ($G = 6\times10^{-4}\ s^{-1}$), but concentrated on the dense data regions (variable weighting function W), is found the best nudging strategy. Indeed, it is better not to force the model too strongly towards mesoscale analyses where we suppose those less accurate.

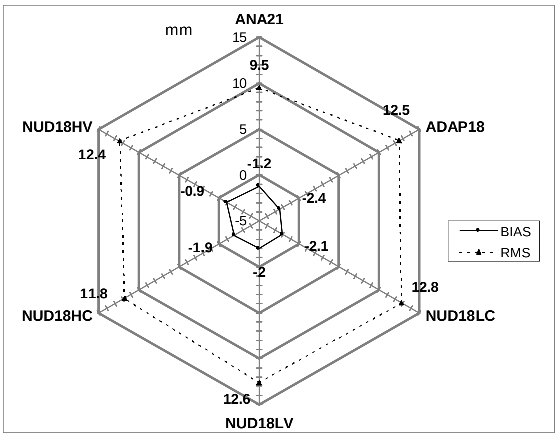


***Figure 3:*** *Same as figure 1 but for experiments ANA21, ADAP18, NUD18LC, NUD18LV, NUD18HC and NUD18HV.*

If we compare with the static initialization experiment that starts from the 21 UTC mesoscale analysis, the bias score for NUD18HV experiment (-0.9 mm) is slightly better (-1.2 mm for ANA21). The amount of precipitation is improved and the maximum of precipitation (136 mm) is really close to the observed one (135 mm) (Figs. 2c,e and 4). However, the precipitation maximum area is better located for the ANA21 experiment (Fig. 2d). Indeed, the maximum precipitation area is a little shifted towards southeast for the NUD18HV experiment, that explains the higher value of rms (Fig. 3).

## 6. CONCLUSION

We have obtained some realistic simulations of a convective event over a French mountainous area by using mesoscale analysis as initial state (ANA22, ANA21, ANA22ADJ). This significantly improves the results compared to initialization from the larger scale operational analysis, due to a better description of the low-level humidity field. The static fine-scale initialization (ANA22ADJ) allows to obtain a better amount and localization of precipitation maximum. The dynamic initialization nudging towards mesoscale analyses gives interesting results too with a very good amount of precipitation. We are currently trying a dynamic fine scale initialization that nudge towards moisture and microphysical fields built from radar data an infrared satellite data. Results will be presented at the conference.

## 7. REFERENCES

Calas, C., V. Ducrocq and S. Sénési, 2000: Mesoscale analyses and diagnostic parameters for deep convection nowcasting, *Met. Applications*, **7**, 143-161.

Ducrocq, V., J.P Lafore, J.L. Redelsperger et F. Orain, 2000: Initialization of a fine scale model for convective system prediction: A case study, *Q. J. Roy. Meteor. Soc.,* **126***, 3041-3066.*

Hoke, J. E., and R.A. Anthes, 1976: The initialization of a three-dimensional models by a dynamic initialization technique. *Mon. Wea. Rev.,* **104**, 1551-1556.

Lafore, J.P *et al*, 1998: The Meso-NH Atmospheric simulation system. Part I: adiabatic formulation and control simulations. *Ann. Geophysicae*, **16**, 90-109.

Ricard, D, V. Ducrocq and J.P. Lafore J.L. 2000: Initialisation à fine échelle pour la modélisation d'épisodes convectifs cévenols. *Atelier de Modélisation de l'Atmosphère. (in french),* 171-174.

Stauffer, D. R., and N. L. Seaman, 1994: Multiscale Four-Dimensional Data Assimilation. *J. Appl. Meteor.,* **33**, 416-434.

Stein, J, E. Richard, J.P. Lafore, J.P. Pinty, N. Asencio And S. Cosma, 2000: High-Resolution Non-Hydrostatic Simulations of Flash-Flood Episodes with grid-nesting and ice-phase parameterization. *Meteor. Atmos. Physics*, **72**, 203-221.

Wang, W and T. T. Warner, 1988: Use of Four-Dimensional Data Assimilation by Newtonian Relaxation and Latent-Heat Forcing to Improve a Mesoscale-Model Precipitation Forecast: A Case Study. *Mon. Wea. Rev.,* **116***, 2593-2613.*

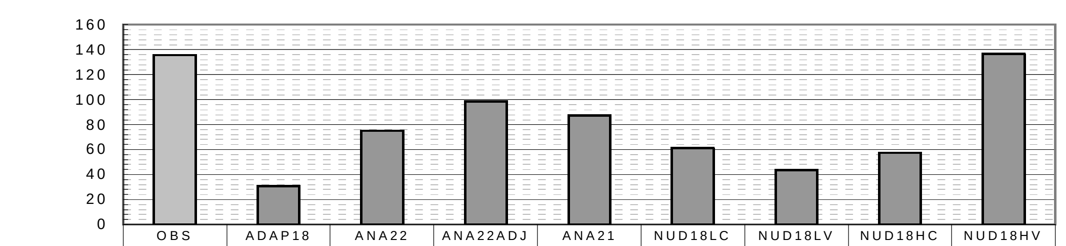


| | OBS | ADAP18 | ANA22 | ANA22ADJ | ANA21 | NUD18LC | NUD18LV | NUD18HC | NUD18HV |
|---|---|---|---|---|---|---|---|---|---|
| MAXIMUM | 135.4 | 30.6 | 74.9 | 98.7 | 87.2 | 61.3 | 43.7 | 57.3 | 136.5 |

***Figure 4:*** *Observed and forecast maximum precipitation totals for 0100-0600UTC 14 October 1995 (in mm).*